Astronomy & Astrophysics manuscript no. aa˙xmm˙XMMUJ004814.0-732204
November 17, 2010

The XMM-Newton survey of the Small Magellanic Cloud: Discovery of the 11.866 s Be/X-ray binary pulsar XMMU J004814.0-732204 (SXP11.87)

R. Sturm[1], F. Haberl[1], M.J. Coe[2], E.S. Bartlett[2], D.A.H. Buckley[3], R.H.D. Corbet[4], M. Ehle[5], M.D. Filipović[6], D. Hatzidimitriou[7,8], S. Mereghetti[9], N. La Palombara[9], W. Pietsch[1], A. Tiengo[9], L.J. Townsend[2], and A. Udalski[10]

[1] Max-Planck-Institut für extraterrestrische Physik, Giessenbachstraße, 85748 Garching, Germany
[2] School of Physics and Astronomy, University of Southampton, Highfield, Southampton SO17 1BJ, United Kingdom
[3] South African Astronomical Observatory, PO Box 9, Observatory 7935, Cape Town, South Africa
[4] University of Maryland, Baltimore County, Mail Code 662, NASA Goddard Space Flight Center, Greenbelt, MD 20771, USA
[5] XMM-Newton Science Operations Centre, ESAC, ESA, PO Box 78, 28691 Villanueva de la Cañada, Madrid, Spain
[6] University of Western Sydney, Locked Bag 1797, Penrith South DC, NSW1797, Australia
[7] Department of Astrophysics, Astronomy and Mechanics, Faculty of Physics, University of Athens, Panepistimiopolis, GR15784 Zografos, Athens, Greece
[8] Foundation for Research and Technology Hellas, IESL, Greece
[9] INAF, Istituto di Astrofisica Spaziale e Fisica Cosmica Milano, via E. Bassini 15, 20133 Milano, Italy
[10] Warsaw University Observatory, Aleje Ujazdowskie 4, 00-478 Warsaw, Poland

Received 21 September 2010 / Accepted 6 November 2010

ABSTRACT

Aims. One of the goals of the XMM-Newton survey of the Small Magellanic Cloud is the study of the Be/X-ray binary population. During one of our first survey observations a bright new transient – XMMU J004814.0-732204 – was discovered.
Methods. We present the analysis of the EPIC X-ray data together with optical observations, to investigate the spectral and temporal characteristics of XMMU J004814.0-732204.
Results. We found coherent X-ray pulsations in the EPIC data with a period of (11.86642 ± 0.00017) s. The X-ray spectrum can be modelled by an absorbed power-law with indication for a soft excess. Depending on the modelling of the soft X-ray spectrum, the photon index ranges between 0.53 and 0.66. We identify the optical counterpart as a B = 14.9mag star which was monitored during the MACHO and OGLE-III projects. The optical light curves show regular outbursts by ∼0.5 mag in B and R and up to 0.9 mag in I which repeat with a time scale of about 1000 days. The OGLE-III optical colours of the star are consistent with an early B spectral type. An optical spectrum obtained at the 1.9 m telescope of the South African Astronomical Observatory in December 2009 shows Hα emission with an equivalent width of 3.5 ± 0.6 Å.
Conclusions. The X-ray spectrum and the detection of pulsations suggest that XMMU J004814.0-732204 is a new high mass X-ray binary pulsar in the SMC. The long term variability and the Hα emission line in the spectrum of the optical counterpart identify it as a Be/X-ray binary system.

Key words. galaxies: individual: Small Magellanic Cloud – galaxies: stellar content – stars: emission-line, Be – stars: neutron – X-rays: binaries

1. Introduction

The Small Magellanic Cloud (SMC) hosts an extraordinary high number of about 80 known Be/X-ray binary systems, compared to the ∼70 known in the Galaxy (as of 2006, Liu et al. 2006) which is a factor of ∼100 more massive than the SMC. Be/X-ray binaries are a subclass of high mass X-ray binaries containing an early type Be donor star with equatorial mass ejection, and an accreting neutron star (NS). Due to the non-spherical and time variable mass ejection these systems show up as X-ray transients, when the NS crosses the disk during the periastron passage, leading to enhanced matter accretion for a few days (type I outbursts). Longer outbursts lasting several weeks (type II) are thought to be caused by expansion of the circumstellar disk (see e.g. Okazaki & Negueruela 2001).

One of the aims of the XMM-Newton (Jansen et al. 2001) large program SMC survey (Haberl & Pietsch 2008a) is the ongoing study of the Be/X-ray binary population of the SMC, which can be used as a star formation tracer for ∼ 50 (30-70) Myr old populations (Antoniou et al. 2010). In this paper we present the analysis of X-ray and optical data from the newly discovered X-ray pulsar XMMU J004814.0-732204.

2. Observations and data reduction

The new transient was discovered on 2009 Oct. 03, during observation 13 (observation ID 0601211301) of the XMM-Newton large program SMC survey. The source was located near the border of CCD 1 (partly spread onto CCD 4) of the EPIC-pn instrument (Strüder et al. 2001) and on CCD 2 of EPIC-MOS2 (Turner et al. 2001). There are no MOS1 data for this source because it was located on CCD 6, which is switched off since XMM-Newton revolution 961. The soft proton background was at a very low level during the whole observation. Therefore, no background screening was necessary, resulting in net exposure

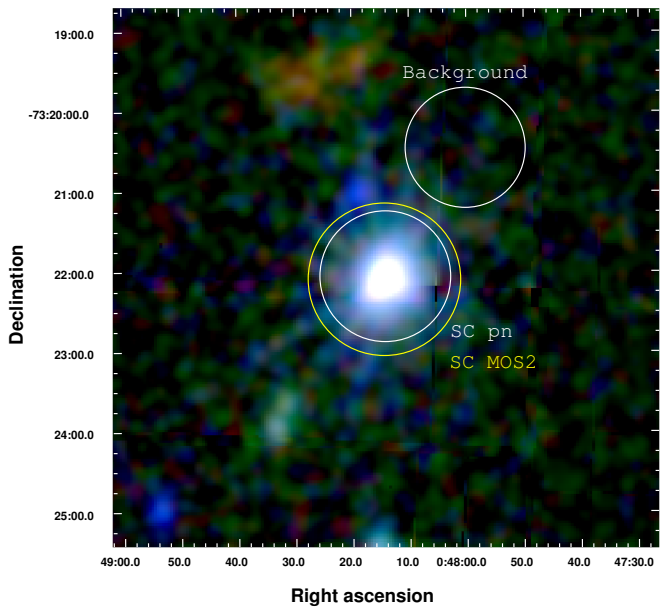

Fig. 1. EPIC colour image of XMMU J004814.0-732204 combining pn and MOS data. The red, green and blue colours represent the X-ray intensities in the 0.2−1.0, 1.0−2.0 and 2.0−4.5 keV energy bands. Circles indicate the extraction regions (with radii of 49″ and 57″ for pn and MOS2 source regions and 45″ for the background).

times of 30779 s and 32368 s for EPIC-pn and EPIC-MOS2, respectively.

We used XMM-Newton SAS 10.0.0 [1] to process the data. We identified sources in the field of view (FoV) for astrometric bore-sight correction by comparison with the Magellanic Clouds Photometric Survey of Zaritsky et al. (2002), obtaining a shift of ΔRA=-0.15″ and ΔDec=-1.23″. The corrected position of the transient as found by `emldetect` is R.A. = $00^h48^m14\overset{s}{.}07$ and Dec. = –73°22′04.″4 (J2000.0), with a statistical error of 0.06″ and a systematic uncertainty of ∼1″ (1 σ confidence for both cases).

For the extraction of EPIC spectra, we selected single-pixel events from the EPIC-pn data (`PATTERN = 0`) and single to quadruple events with `PATTERN≤12` from EPIC-MOS2 data, both with `FLAG = 0`. The SAS task `eregionanalyse` was used to determine circular source extraction regions by optimizing the signal to noise ratio as shown in Fig. 1. We ensured that the source extraction region has a distance of >10″ to other detected sources. For the background extraction region, we chose a circle in an area free of point sources and on the same CCD as the source for both instruments. The EPIC-pn and EPIC-MOS2 spectra contain 9286 and 8054 background subtracted counts, respectively, and were binned to a minimum signal-to-noise ratio of 5 for each bin. For the timing analysis, we used also double-pixel events for EPIC-pn. To increase the statistics for the timing analysis we also generated a merged event list from both instruments, containing 25945 cts (source + background).

[1] Science Analysis Software (SAS), http://xmm.esac.esa.int/sas/

3. X-ray data analysis and results

3.1. Spectral analysis of the X-ray data

We used `XSPEC` (Arnaud 1996) version 12.5.0x for spectral fitting. The two EPIC spectra were fitted simultaneously with a common set of spectral model parameters, only a relative normalisation factor was allowed to vary to account for instrumental differences. The spectrum (Fig. 2) was modelled first with an absorbed power-law. We fixed the Galactic photo-electric absorption at a column density of $N_{H,GAL} = 6{\times}10^{20}$ cm^{-2} with abundances according to Wilms et al. (2000), whereas the SMC column density was a free parameter with abundances for elements heavier than Helium fixed at 0.2. The best-fit parameters are summarised in Table 1 where errors denote 90% confidence ranges.

The extraction for the EPIC-pn spectrum is hampered by the CCD gap cutting the extraction region. The missing area is taken into account in the calculation of the effective area by `arfgen`. However, we noticed that when using the default spatial resolution (parameter badpixelresolution=2.0″) the flux derived from the EPIC-pn spectrum is higher by (21 ± 3)% than compared to MOS. Using badpixelresolution=1.0″ reduces the flux discrepancy to 7%, which is within the expected systematic uncertainties in the presence of gaps. Extracting the EPIC-pn spectrum from a smaller source region with radius 6″, so that the complete source region is placed on CCD 1, yields a flux that only differs by ∼1% from the MOS2 value. The spectral shape is not affected by the CCD gap, but the number of source counts for the smaller extraction region is a factor of two lower.

In principle, this fit is formally acceptable and additional components are not required. However, soft excesses and fluorescent emission from iron are known to contribute to the X-ray emission of some Be X-ray binaries (e.g. Eger & Haberl 2008; La Palombara et al. 2009; Hickox et al. 2004). To investigate these possibilities we first added a black-body emission component to the model (Table 1). This component contributes ∼2% to the observed flux and ∼3% to the absorption corrected luminosity. For the bolometric luminosity we obtained $(1.40{\pm}0.35){\times}10^{35}$ erg s^{-1}. Compared to the single power-law the reduced χ^2 improved from 1.09 to 1.01, which corresponds to a F-test chance probability of 2.6×10^{-10} and formally proves the significance of this component (but see Protassov et al. 2002, for limitations of the F-test). An additional emission line with fixed energy at 6.4 keV and unresolved line width (fixed at 0), yielded a line flux of $4.6 \pm 4.0 \times 10^{-6}$ photons cm^{-2} s^{-1} corresponding to an equivalent width given in Table 1. Substituting the 6.4 keV line by a 6.7 keV line for ionized Fe XXV resulted in an upper limit for the equivalent width of 41 eV.

If we replace the black-body component by a multi-temperature disk black-body model (diskbb in `XSPEC`), we derive a lower limit for the inner disk radius of $R_{\rm in} = 5.9^{+3.5}_{-2.2}$ km (for a disk inclination of $\Theta = 0$ with $R_{\rm in} \propto 1/\sqrt{cos\Theta}$). Following Hickox et al. (2004) to estimate the inner disk radius we infer $R_{\rm in} = \sqrt{L_{\rm X}/(4\pi\sigma T^4)} = 39$ km.

3.2. Timing analysis of the X-ray data

We corrected the event arrival times to the solar system barycentre using the SAS task `barycen` and searched for periodicities in the X-ray light curves using fast Fourier transform (FFT) and light curve folding techniques. The power density spectra derived from light curves in various energy bands from both EPIC instruments showed a periodic signal at 0.084 Hz. To in-

Table 1. Spectral fit results.

Model[1]	SMC N_H [10^{21}cm^{-2}]	γ	kT [eV]	R[2] [km]	EW_{Fe} [eV]	Flux[3] [erg cm^{-2} s^{-1}]	L_x[4] [erg s^{-1}]	χ^2/dof
PL	1.72±0.25	0.66±0.03	–	–	–	(9.0±0.3)×10^{-12}	4.0×10^{36}	570/523
PL+BB	2.32±0.44	0.52±0.05	279±43	12.2±1.4	–	(9.3±0.5)×10^{-12}	4.2×10^{36}	524/521
PL+BB+Fe-line	2.34±0.45	0.53±0.05	277±40	12.2±1.4	35±30	(9.6±0.5)×10^{-12}	4.2×10^{36}	520/520
PL+DiskBB	2.99±0.54	0.52±0.06	383±97	>5.9±3.5	–	(9.3±0.7)×10^{-12}	4.2×10^{36}	528/521

[1] For definition of spectral models see text. [2] Radius of the emitting area (for BB) or inner disk radius (DiskBB, for the definition see text). [3] Observed 0.2-10.0 keV flux. [4] Source intrinsic X-ray luminosity in the 0.2-10.0 keV band (corrected for absorption) for a distance to the SMC of 60 kpc (Hilditch et al. 2005).

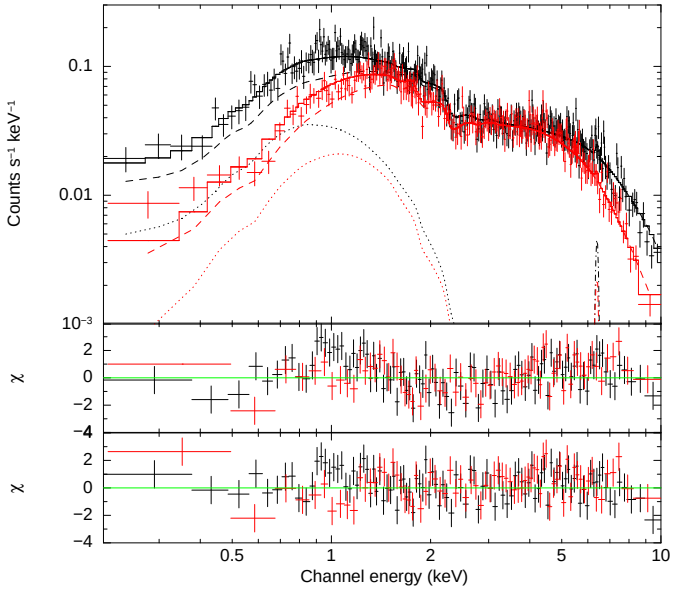

Fig. 2. EPIC spectra of XMMU J004814.0-732204. The top panel shows the EPIC-pn (black) and EPIC-MOS2 (red) spectra together with the best-fit model (solid line) of an absorbed power-law (dashed line) plus black-body (dotted line) and iron fluorescent line (dash-dotted line). The residuals (for better comparison they are re-binned by an additional factor of three) are plotted for this model (bottom panel) and for the best-fit single power-law model (middle panel).

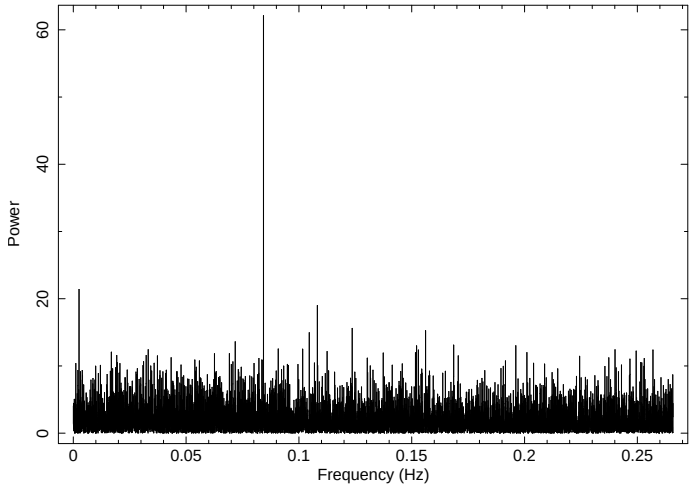

Fig. 3. Power density spectrum created from the merged EPIC-pn and EPIC-MOS2 data in the 0.2-10.0 keV energy band. The time binning of the input light curve is 1.882 s.

crease the signal to noise ratio, we then created light curves from the merged event list of EPIC-pn and EPIC-MOS2 (delimited to common time intervals). Figure 3 shows the inferred power density spectrum from the 0.2-10.0 keV energy band with the clear peak at a frequency of 0.084 Hz. Following Haberl et al. (2008) we used a Bayesian periodic signal detection method (Gregory & Loredo 1996) to determine the pulse period with 1σ error to (11.86642 ± 0.00017) s. The pulse profiles folded with this period in the EPIC standard energy bands (0.2-0.5 keV, 0.5-1.0 keV, 1.0-2.0 keV, 2.0-4.5 keV and 4.5-10 keV) are plotted in Fig. 4 together with hardness ratios derived from the pulse profiles in two adjacent energy bands ($HR_i = (R_{i+1} - R_i)/(R_{i+1} + R_i)$ with R_i denoting the background-subtracted count rate in energy band i (with i from 1 to 4). Assuming a sinusoidal pulse profile, we determined a pulsed fraction of (7.5 ± 1.0)% for the 0.2−10.0 keV band. The profiles suggest some evolution from a single-peaked to a double-peaked structure with increasing energy, causing the variations in hardness ratios HR3 and HR4. A strong dependence of the pulse profiles on energy (e.g. Wilson et al. 2003; Haberl et al. 2008) and luminosity (e.g. Bildsten et al. 1997) is seen from a number of high mass X-ray binaries.

3.3. Long-term X-ray variability

The position of XMMU J004814.0-732204 was covered in two previous XMM-Newton observations on 2000 Oct. 15 (ObsID: 0110000101) and 2007 Apr. 11 (ObsID: 0404680301) with a background-screened net exposure of 21.6 ks and 17.6 ks, respectively. In the latter observation the source position was only covered by the MOS2 FoV. In both observations, no source was detected above a likelihood threshold of 6. Using sensitivity maps we derived 3σ upper limits of 2.5×10^{-3} cts s^{-1} and 2.7×10^{-3} cts s^{-1}, respectively. Assuming the same spectrum as during the outburst, this corresponds to a flux limit of 1.7×10^{-14} erg cm^{-2} s^{-1} (from Oct. 2000, measured by EPIC-pn) and 6.1×10^{-14} erg cm^{-2} s^{-1} (Apr. 2007, EPIC-MOS2) in the 0.2 – 10.0 keV band and to luminosity limits of 7.6×10^{33} erg s^{-1} and 2.7×10^{34} erg s^{-1}, respectively.

Also in a Chandra (Weisskopf et al. 2000) ACIS-I observation (Observation ID 2945) on 2002 Oct. 2 this position was covered with a 11.8 ks exposure, and no source was detected. We used the CIAO (Version 4.2) task `aprates` to estimate a 3σ upper limit of 5.1×10^{-4} cts s^{-1}. Assuming the same spectrum as above, this corresponds to a flux limit of 1.6×10^{-14} erg cm^{-2} s^{-1} in the 0.2 – 10.0 keV band (luminosity of 7.1×10^{33} erg s^{-1}).

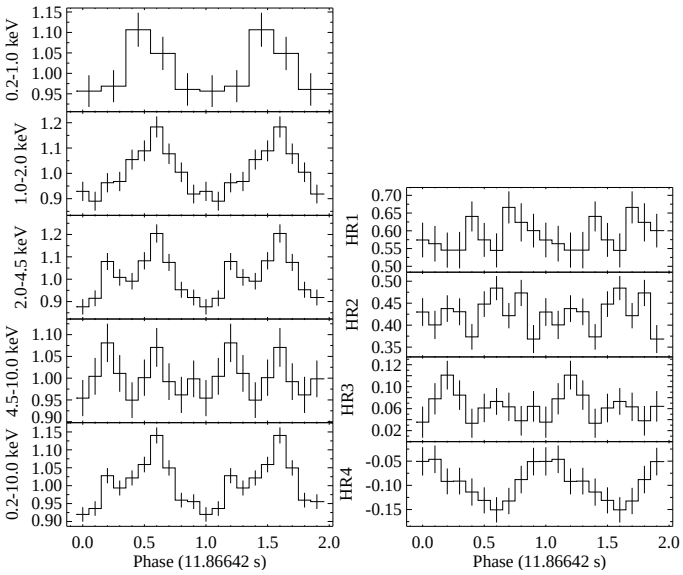

Fig. 4. Left: Pulse profiles obtained from the merged EPIC data in different energy bands (for better statistics the first two standard energy bands were combined in the top panel, the bottom panel shows all five energy bands combined). The profiles are background-subtracted and normalized to the average count rate (0.116, 0.228, 0.249, 0.207 and 0.801 cts s^{-1}, from top to bottom. Right: Hardness ratios as a function of pulse phase derived from the pulse profiles in two neighbouring standard energy bands

The upper limits from the XMM-Newton and Chandra observations show that XMMU J004814.0-732204 increased in brightness at least by a factor of 560 during its outburst.

RXTE monitoring of the SMC has been carried out for nearly a decade (Galache et al. 2008) and XMMU J004814.0-732204 has frequently fallen within the pointing direction of the telescope, often at a collimator response of ≥60%. Unfortunately, the time of the XMM-Newton detection on MJD 55107 falls into the gap in the RXTE monitoring (MJD 55080 - 55138) when the spacecraft was temporarily disabled, so there is no simultaneous RXTE coverage. Within the envelope of the last 9.5 years there are no possible detections of this source in the periods of time (approximately 6.5 years) when the source was above a 0.6 collimator response. The RXTE pulse monitoring is sensitive to detections with a pulsed amplitude in excess of 0.15-0.2 cts/s/PCU. This approximately translates into ∼0.5-1.0 cts/s/PCU - depending on the collimator response and pulsed fraction (which is not very high for XMMU J004814.0-732204) - or a luminosity limit of $\sim 2\times10^{36}$ erg s^{-1} for a source in the SMC.

4. Optical data

4.1. Identification of the optical counterpart

Searching optical catalogues of Zaritsky et al. (2002), MACHO and OGLE, we found three stars which are located within the 3σ error radius around the XMM-Newton position. Their positions and magnitudes from Zaritsky et al. (2002) and their OGLE-II and MACHO entries are listed in Table 2. A finding chart produced from OGLE-III data is shown in Fig. 5.

The star closest to the X-ray position (OGLE-III 14642) has colours and brightness consistent with an early B star. Its position on the U-B vs. B-V diagram of Be stars (e.g. Fig. 1 of Feinstein & Marraco 1979) is also entirely consistent with it being a Be star. The same holds for the reddening-free Q-index of -0.85 (Johnson & Morgan 1955; Massey et al. 2007). This candidate also appears as number 10287 in the survey list of Massey (2002). The (B-V) colour index from that catalogue is (B-V)=-0.12±0.01. Correcting for an extinction to the SMC of E(B-V)=0.09 (Schwering & Israel 1991, also used for our spectral type estimates hereafter) gives an intrinsic colour of (B-V)=-0.21±0.01. From Wegner (1994) this indicates a spectral type in the range B1.5V - B2.5V - typical of optical counterparts to Be/X-ray binaries in the SMC (McBride et al. 2008). However, care must always be taken when interpreting colour information as a spectral type in systems that clearly have circumstellar disks contributing some signal to the B and V bands.

Optical photometry was performed at the Faulkes Telescope South (FTS) on 25 November 2009 (MJD 55160). The telescope is located at Siding Spring, Australia and is a 2m, fully autonomous, robotic Ritchey-Chrètien reflector on an alt-azimuth mount. The telescope employs a Robotic Control System (RCS). The telescope was used in Real Time Interface mode for the observation of XMMU J004814.0-732204. All the observations were pipeline-processed (flat-fielding and de-biasing of the images). The I-band magnitude of the optical counterpart was determined to be 15.30±0.02 mag by comparison with several other nearby stars on the same image frame and in the OGLE database. These comparison stars have not exhibited any significant variability in the last 8 years of OGLE monitoring.

Figure 6 shows optical and IR photometry of OGLE-III 14642 taken at the different epochs - see Table 3 for the actual values. The earliest optical data come from Massey (2002) and were recorded on 1999 Jan. 8. These data are combined with IR measurements taken on 2002 Aug. 31 with the Sirius camera on the 1.5m IRSF telescope in South Africa (Kato et al. 2007). Also included is the OGLE I band measurement taken simultaneously with the Sirius IR data set. These early data are compared to a B, V, R & I photometric data set recorded on 2009 Nov. 25 from the FTS.

For comparison, a stellar atmosphere model (Kurucz 1979) representing a B2V star (T_{eff} = 22,000 K and log(g) = 4.0) is also shown where the model has been normalised to the most recent B band measurement. It is very clear that the recent data taken around the time of the XMM-Newton detection represent the source in a much lower activity state than the earlier data. Furthermore, the shape of the model atmosphere indicates clear evidence for the presence of a significant IR excess in the past, almost certainly arising from the circumstellar disk of the system. But in late 2009 the disk had diminished significantly, to the extent that there is little in the way of IR excess - this is supported by the very weak Hα emission (see Section 4.3 below).

The star OGLE-III 14688 is probably a red (K to M) giant from its OGLE colours. The light curve shows small variations of the order of 0.1 mag in the I-band, but no evidence for any coherent fluctuations. There is an object from the Two Micron All Sky Survey (Skrutskie et al. 2006) – 2MASS J00481347-7322030 – which is closest to the position of this star, with J=14.76, H=14.13, K=14.04, J-H=0.63 and H-K=0.09, which rather points towards a K2 star.

The third object (OGLE-III 14689) is likely a late B-type star (B5-B9) from the OGLE colours. The light curve shows fluctuations of the order of 0.05 mag in the I band and evidence for a strong modulation at a period of 2.19 days. The folded light curve appears sinusoidal which is probably evidence for non-radial pulsations in the star (Diago et al. 2008).

Table 2. Possible optical counterparts of XMMU J004814.0-732204.

RA(2000)[a]	DEC(2000)[a]	dist.[b]	U (mag)[a]	B (mag)[a]	V (mag)[a]	I (mag)[a]	Q (mag)[c]	OGLE-III	MACHO
00 48 14.10	-73 22 03.6	0.″76	13.96±0.03	14.90±0.02	15.02±0.05	15.25±0.13	-0.85±0.05	14642	212.15846.31
00 48 13.52	-73 22 02.8	2.″86	–	18.90±0.07	17.26±0.07	15.88±0.04	–	14688	212.15846.83
00 48 13.78	-73 22 00.5	4.″07	15.20±0.03	15.93±0.03	15.90±0.03	16.00±0.04	-0.75±0.05	14689	212.15846.70

[a]according to Zaritsky et al. (2002).
[b]distance of the Zaritsky et al. (2002) positions to the bore-sight corrected XMM-Newton position.
[c]Reddening-free Q-index = (U-B) − 0.72 × (B-V).

Table 3. Optical and IR photometry of OGLE-III 14642

	M2002[a] 1998 Jan 8 MJD 51186	K2007[b] 2002 Aug 31 MJD 52517	FTS[c] 2009 Nov 25 MJD 55160	Sirius[c] 2009 Dec 15 MJD 55180
B	14.54±0.01	–	14.87±0.20	–
V	14.66±0.01	–	14.86±0.03	–
R	14.66±0.01	–	14.87±0.03	–
I	–	14.70±0.01	15.30±0.02	–
J	–	14.67±0.01	–	15.46±0.01
H	–	14.62±0.01	–	15.47±0.02
K	–	14.53±0.02	–	15.49±0.07

[a]Massey (2002). [b]Kato et al. (2007). [c]This work.

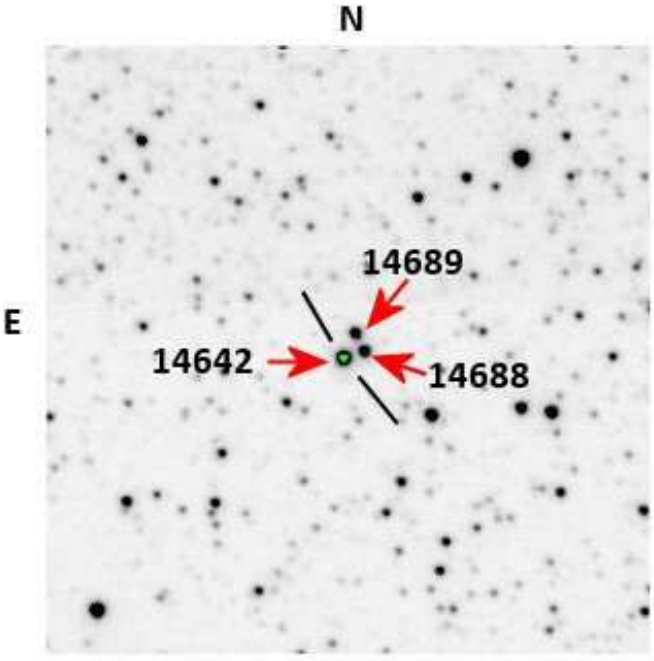

Fig. 5. Finding chart of SXP11.87. The I band image from OGLE-II shows the 3 close objects near the X-ray position marked with their OGLE-III identification (arrows). The two lines further mark the likely counter part. The image size is 1.′5 by 1.′5.

The position, optical magnitudes and colours make the star closest to the X-ray position (OGLE-III 14642) the most likely counterpart.

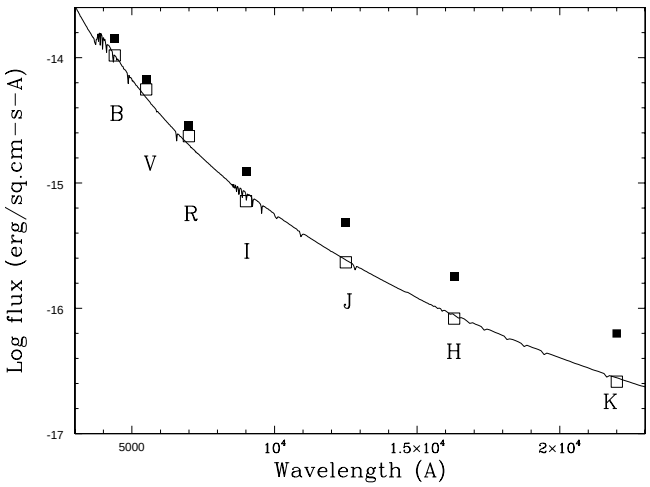

Fig. 6. Combined optical-IR flux for our counterpart OGLE-III 14642 at two epochs. (a) a historical data set (1999-2002) - solid symbols; (b) data set from the time of outburst (Nov-Dec 2009) - open symbols. See text for details of the observations. Both data sets are compared to a Kurucz model atmosphere for a B2V star in which this stellar model has been normalised to the outburst B band point.

4.2. Long-term variability of OGLE-III 14642

The identification of XMMU J004814.0-732204 with OGLE-III 14642 is supported by the MACHO and OGLE light curves. This star shows strong outbursts repeating on time scales of ∼1000 days. Fig. 7 shows the light curves of the proposed optical counterpart in approximate B and R magnitudes derived from MACHO data (ID 212.15846.31) and in the I-band from OGLE-II and OGLE-III. The I-band data point which we obtained at FTS was added to the OGLE light curve. The MACHO light curve shows two outbursts around April 1995 and Jan. 1998, while OGLE observed six consecutive outbursts between June 1997 and Dec. 2008.

The X-ray flux of the source is not obviously correlated with the optical outburst activity. The first XMM-Newton non-detection was during maximum optical brightness. The Chandra non-detection was close to the maximum optical brightness, the last XMM-Newton non-detection later in the optical decline, while the detection could have happened at the decline or already in optical low-state (see Fig. 7).

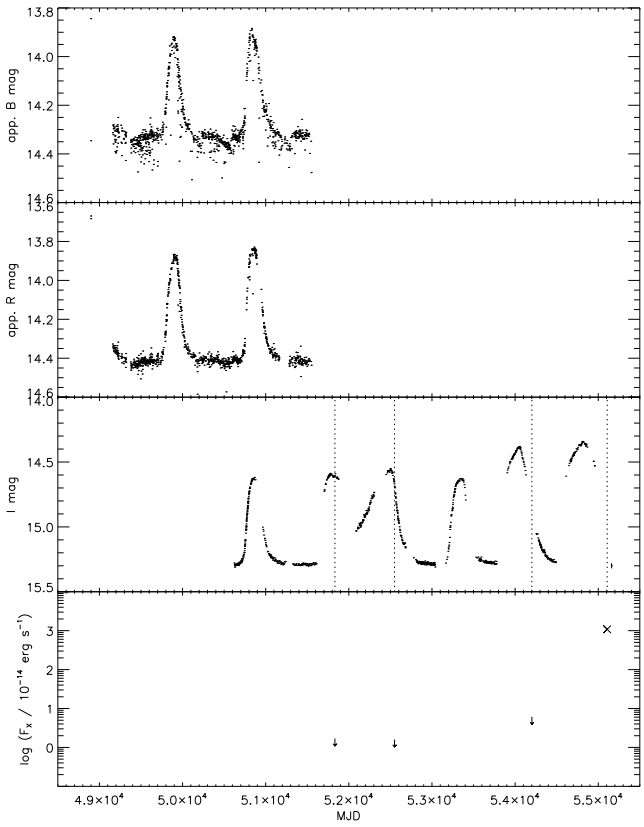

Fig. 7. Multi-wavelength light curves of the XMMU J004814.0-732204 / OGLE-III 14642 system. The upper two panels show the MACHO B- and R-band. In the third panel the OGLE-III I-band light curve is plotted, with the last data point indicating our own measurement using the Faulkes telescope (see text). Dashed lines indicate the times of X-ray measurements, as shown in the bottom panel. Arrows mark upper limits (XMM-Newton, Chandra and XMM-Newton in chronological order, see Sect. 3.3), the cross indicates the XMM-Newton detection.

4.3. Optical spectrum

Spectroscopic observations of the Hα region were made on 11 Dec. 2009 (MJD 55176) using the 1.9 m telescope of the South African Astronomical Observatory (SAAO). A 1200 lines per mm reflection grating blazed at 6800 Å was used with the SITe CCD which is effectively 266×1798 pixels in size, creating a wavelength coverage of 6200 Å to 6900 Å. The pixel scale in this mode was 0.42 Å/pixel. The data were reduced using IRAF standard routines and the resulting spectrum is shown in Fig. 8. The peak is at 6566 Å which is consistent with the corresponding rest wavelength of the Hα line corrected for the motion of the SMC. In this mode the spectral resolution is ∼0.2 nm for the signal to noise of ∼ 10. We measured an Hα line emission width of EW = 3.5 ± 0.6 Å, the error being calculated using the prescription given in Howarth & Phillips (1986).

5. Discussion and Conclusions

One of the first XMM-Newton observations of the SMC survey revealed the new high mass X-ray binary pulsar XMMU J004814.0-732204 with a pulse period of 11.866 s (following Coe et al. 2005, we give it the alternative name SXP11.87). Its X-ray behaviour and the properties of the optical counterpart (star with OGLE-III ID 14688) are typical for a Be - neutron star binary system. In particular the appearance as an X-ray transient (a factor of at least 560 brighter during the outburst on Oct. 2009 as compared to non-detections from archival XMM-Newton and Chandra observations), the hard power-law shape of the X-ray spectrum, the pulse period, the optical brightness, variability and colours (indicating an early B star) and finally the Hα emission line in the optical spectrum clearly confirm XMMU J004814.0-732204 as another Be/X-ray binary in the SMC.

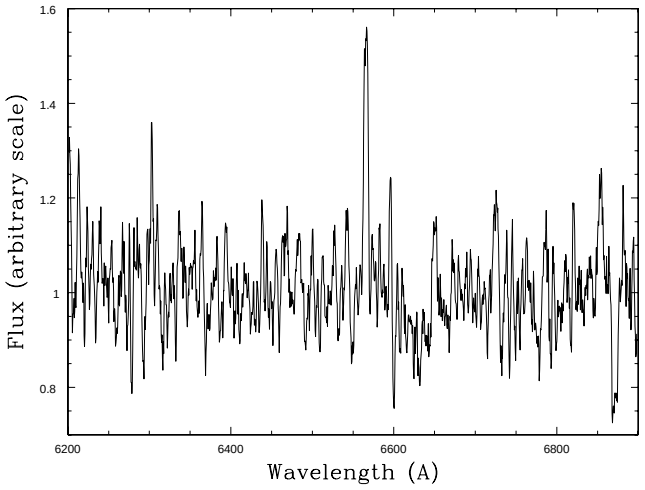

Fig. 8. Hα spectrum of the OGLE optical candidate #14642 taken 11 Dec. 2009 at SAAO.

The power-law photon index derived from the EPIC spectra of 0.53−0.66 (depending on the spectral modelling of the soft part of the spectrum by including an additional soft model component or not) is on the hard side of the distribution of photon indices for Be/X-ray binaries in the SMC, which shows a maximum at ∼0.9−1.0 (Haberl et al. 2008; Haberl & Pietsch 2004). The range of values obtained for XMMU J004814.0-732204 is similar to the index of 0.35−0.54 reported for the 6.85 s pulsar XTE J0103−728 (also using XMM-Newton data in the same energy band; Haberl & Pietsch 2008b). It should be noted, that the latter, also called SXP6.85, was detected at energies up to 35 keV with RXTE and INTEGRAL during a long type II outburst (Townsend et al. 2010) showing that the hard spectrum extends to energies beyond the sensitivity of XMM-Newton. SXP11.87 and SXP6.85 also show similarities in their spectra at energies below 2 keV, indicating a soft X-ray excess. However, the energy resolution of the CCD instruments is not sufficient to determine the exact nature of this component. Some constraints can be inferred by using different models for the soft component. If one assumes a black-body component, a temperature of ∼280 eV and black-body radius of ∼13.4 km is derived for SXP11.87. While this could still be compatible with the size of the neutron star, the corresponding black-body radius for SXP6.85 is too large (30 km, Haberl & Pietsch 2008b). Therefore, these authors conclude that the soft excess more likely originates near the inner edge of an accretion disk as expected for intermediate X-ray luminosities. The very similar parameters derived for a soft excess emission suggest the same picture for SXP11.87, although the inferred black-body or inner disk radii seem to be smaller than the corresponding values for SXP6.85. However, also emission

by diffuse gas through collisional heating or photoionisation is possible for both cases (Hickox et al. 2004).

The MACHO and OGLE light curves of the optical counterpart of XMMU J004814.0-732204 show prominent outbursts repeating on a time scale of about 1000 days. Very similar behaviour was reported from the optical counterpart of the 18.37 s Be/X-ray binary pulsar XMMU J004911.4-724939 which showed two outbursts separated by about 1300 days in MACHO and OGLE-I data (Haberl et al. 2008). Such outburst behaviour is also observed from other (single) Be stars (Mennickent et al. 2002). Because of this and the fact that the outbursts do not repeat strictly periodically, it is unlikely that they are related to the orbital period of the binary system. Moreover, from the Corbet relation between neutron star spin period and the orbital period (Corbet 1984) a much shorter orbital period of about 20−200 days is expected (see Laycock et al. 2005; Corbet et al. 2009, for more recent versions of the P_s/P_{orb} diagram).

Acknowledgements. The XMM-Newton project is supported by the Bundesministerium für Wirtschaft und Technologie/Deutsches Zentrum für Luft- und Raumfahrt (BMWI/DLR, FKZ 50 OX 0001) and the Max-Planck Society. R.S. acknowledges support from the BMWI/DLR grant FKZ 50 OR 0907. S.M., N.L. and A.T. acknowledge the support of ASI through contract I/088/06/0. L.J.T. is in receipt of a University of Southampton Mayflower Scholarship. A.U. acknowledges support from the MNiSW/BST grant.

References

Antoniou, V., Zezas, A., Hatzidimitriou, D., & Kalogera, V. 2010, ApJ, 716, L140
Arnaud, K. A. 1996, in Astronomical Society of the Pacific Conference Series, Vol. 101, Astronomical Data Analysis Software and Systems V, ed. G. H. Jacoby & J. Barnes, 17
Bildsten, L., Chakrabarty, D., Chiu, J., et al. 1997, ApJS, 113, 367
Coe, M. J., Edge, W. R. T., Galache, J. L., & McBride, V. A. 2005, MNRAS, 356, 502
Corbet, R. H. D. 1984, A&A, 141, 91
Corbet, R. H. D., Coe, M. J., McGowan, K. E., et al. 2009, in IAU Symposium, Vol. 256, IAU Symposium, ed. J. T. van Loon & J. M. Oliveira, 361–366
Diago, P. D., Gutiérrez-Soto, J., Fabregat, J., & Martayan, C. 2008, A&A, 480, 179
Eger, P. & Haberl, F. 2008, A&A, 491, 841
Feinstein, A. & Marraco, H. G. 1979, AJ, 84, 1713
Galache, J. L., Corbet, R. H. D., Coe, M. J., et al. 2008, ApJS, 177, 189
Gregory, P. C. & Loredo, T. J. 1996, ApJ, 473, 1059
Haberl, F., Eger, P., & Pietsch, W. 2008, A&A, 489, 327
Haberl, F. & Pietsch, W. 2004, A&A, 414, 667
Haberl, F. & Pietsch, W. 2008a, in X-rays From Nearby Galaxies, ed. S. Carpano, M. Ehle, & W. Pietsch, 32–37
Haberl, F. & Pietsch, W. 2008b, A&A, 484, 451
Hickox, R. C., Narayan, R., & Kallman, T. R. 2004, ApJ, 614, 881
Hilditch, R. W., Howarth, I. D., & Harries, T. J. 2005, MNRAS, 357, 304
Howarth, I. D. & Phillips, A. P. 1986, MNRAS, 222, 809
Jansen, F., Lumb, D., Altieri, B., et al. 2001, A&A, 365, L1
Johnson, H. L. & Morgan, W. W. 1955, ApJ, 122, 142
Kato, D., Nagashima, C., Nagayama, T., et al. 2007, PASJ, 59, 615
Kurucz, R. L. 1979, ApJS, 40, 1
La Palombara, N., Sidoli, L., Esposito, P., Tiengo, A., & Mereghetti, S. 2009, A&A, 505, 947
Laycock, S., Corbet, R. H. D., Coe, M. J., et al. 2005, ApJS, 161, 96
Liu, Q. Z., van Paradijs, J., & van den Heuvel, E. P. J. 2006, A&A, 455, 1165
Massey, P. 2002, ApJS, 141, 81
Massey, P., McNeill, R. T., Olsen, K. A. G., et al. 2007, AJ, 134, 2474
McBride, V. A., Coe, M. J., Negueruela, I., Schurch, M. P. E., & McGowan, K. E. 2008, MNRAS, 388, 1198
Mennickent, R. E., Pietrzyński, G., Gieren, W., & Szewczyk, O. 2002, A&A, 393, 887
Okazaki, A. T. & Negueruela, I. 2001, A&A, 377, 161
Protassov, R., van Dyk, D. A., Connors, A., Kashyap, V. L., & Siemiginowska, A. 2002, ApJ, 571, 545
Schwering, P. B. W. & Israel, F. P. 1991, A&A, 246, 231
Skrutskie, M. F., Cutri, R. M., Stiening, R., et al. 2006, AJ, 131, 1163
Strüder, L., Briel, U., Dennerl, K., et al. 2001, A&A, 365, L18
Townsend, L. J., Coe, M. J., McBride, V. A., et al. 2010, MNRAS, 403, 1239
Turner, M. J. L., Abbey, A., Arnaud, M., et al. 2001, A&A, 365, L27
Wegner, W. 1994, MNRAS, 270, 229
Weisskopf, M. C., Tananbaum, H. D., Van Speybroeck, L. P., & O'Dell, S. L. 2000, in Presented at the Society of Photo-Optical Instrumentation Engineers (SPIE) Conference, Vol. 4012, Society of Photo-Optical Instrumentation Engineers (SPIE) Conference Series, ed. J. E. Truemper & B. Aschenbach, 2–16
Wilms, J., Allen, A., & McCray, R. 2000, ApJ, 542, 914
Wilson, C. A., Finger, M. H., Coe, M. J., & Negueruela, I. 2003, ApJ, 584, 996
Zaritsky, D., Harris, J., Thompson, I. B., Grebel, E. K., & Massey, P. 2002, AJ, 123, 855